Available online at www.sciencedirect.com
ScienceDirect
Geochimica et Cosmochimica Acta 70 (2006) 5270–5284
Geochimica
www.elsevier.com/locate/gca

Uranyl sorption species at low coverage on Al-hydroxide: TRLFS and XAFS studies

A. Froideval [a], M. Del Nero [a,*], C. Gaillard [a], R. Barillon [a], I. Rossini [a], J.L. Hazemann [b]

[a] *Institut Pluridisciplinaire Hubert Curien, Département de Recherches Subatomiques, ULP / CNRS / IN2P3, UMR 7500, 67037 Strasbourg Cedex 2, France*
[b] *Laboratoire de Cristallographie, CNRS, UPR 5031, 38042 Grenoble Cedex 9, France*

Received 21 March 2006; accepted in revised form 8 August 2006

Abstract

Detailed understanding of the respective roles of solution and surface parameters on the reactions at uranyl solution/Al-(hydr)oxide interfaces is crucial to model accurately the behaviour of U in nature. We report studies on the effects of the initial aqueous uranyl speciation in moderately acidic solutions, e.g. of mononuclear, polynuclear uranyl species and/or (potential) U(VI) colloids, on the sorption of U by large surface areas of amorphous Al-hydroxide. Investigations by Extended X-ray Absorption Fine Structure (EXAFS) and Time-Resolved Laser-induced Fluorescence Spectroscopy (TRLFS) reveal similar U coordination environments on Al-hydroxide for low to moderate U loadings of sorption samples obtained at pH 4–5, independently of the presence of mononuclear or polynuclear aqueous species, or of the potential instability of initial solutions favoring true U-colloids formation. EXAFS data can be interpreted in terms of a dimeric, bidentate, inner-sphere uranyl surface complex as an average of the U surface structures. TRLFS data, however, provide valuable insights into the complex U surface speciation. They indicate multiple uranyl surface species under moderately acidic conditions, as predominant mononuclear and/or dinuclear, inner-sphere surface complexes and as additional minor species having U atoms in a uranyl (hydr)oxide-like coordination environment. The additional species probably occur as surface polymers and/or as adsorbed true U colloids, depending on the aqueous U concentration level (1–100 μM). These results are of importance because they suggest that Al-hydroxide surface characteristics strongly control uranyl surface species in moderately acidic systems.

1. Introduction

The mining and reprocessing of natural U and the past waste disposal activities have generated contaminated soils and sediments, as well as U mill tailings which produce acidic-water contamination plumes (e.g. Morrison et al., 1995; Arnold et al., 1998). Uranium in hexavalent oxidation state, i.e. uranyl UO_2^{2+}, is stable in many soil and aquifer systems and tends to generate potentially mobile U(VI)-carriers, such as hydrolysis products, complex ions, true and pseudo colloids. Sorption mechanisms onto minerals, such as adsorption and co-precipitation, have been suggested to retard the migration of U in specific ecosystems (e.g. Payne et al., 1994; Murakami et al., 1997; Bruno et al., 1998; Del Nero et al., 1999, 2004 Bruno et al., 2002). In particular, sorption of uranyl onto aluminium (hydr)oxides is of interest due to the abundance of such minerals in nature, to their high specific surface area, and to their high surface affinity for U(VI). The knowledge of the reactions of uranyl ions at the Al-(hydr)oxide/colloid/solution interfaces is thus of importance for predicting U geo-cycling.

Several authors have found evidence, by using Extended X-ray Absorption Fine Structure (EXAFS) spectroscopy, that U(VI) forms mononuclear, inner-sphere, bidentate uranyl complexes at Fe-oxide surfaces, in systems equilibrated at acidic or basic pH ($4 < pH_F < 8$) with 10–100 μM initial uranyl solutions that contain a range of mononuclear and polynuclear species (Waite et al., 1994; Reich et al., 1998; Bargar et al., 2000). Reich et al. (1996, 1998) and Sylwester et al. (2000) have shown by EXAFS

* Corresponding author. Fax: +33 3 88 10 64 31.
E-mail address: mireille.delnero@ires.in2p3.fr (M. Del Nero).

0016-7037/$ - see front matter © 2006 Elsevier Inc. All rights reserved.
doi:10.1016/j.gca.2006.08.027

that UO_2^{2+} ions sorbed at pH 3.5 also form such complexes at Al-oxide and silica(te) surfaces. Sylwester et al. (2000) have pointed to the additional formation of polymeric surface species at near-neutral pH, when the covering by U (Γ) of silica and alumina surfaces is increased up to $\Gamma \approx 0.1$ and $\Gamma \approx 0.5$ μmol U/m^2 solid, respectively, for initial solution concentrations ($[U]_{I_{AQ}}$) of ~40 μM.

The formation of multiple uranyl surface species onto alumina, silica and silicate surfaces has been suggested by the use of spectroscopic techniques able to detect distinct U coordination environments, i.e. Time-Resolved Laser-induced Fluorescence Spectroscopy (TRLFS) and X-ray Photoelectron Spectroscopy (XPS). Gabriel et al. (2001) have evidenced, for uranyl sorbed at trace concentration level onto silica, three pH-dependent fluorescent species postulated as distinct mononuclear, bidentate, inner-sphere uranyl surface complexes. At moderate to high U surface coverage of quartz ($1 < \Gamma < 15$ μmol U/m^2), two pH-dependent uranyl surface components have been detected by XPS (Froideval et al., 2003; Froideval, 2004). The XPS results have been interpreted in terms of mononuclear, inner-sphere U surface complexes coexisting with polynuclear/schoepite-like surface species, irrespective of solution parameters favouring either mononuclear or polynuclear/colloïdal U(VI) species in solution ($3 \leqslant pH_F \leqslant 8$; $10\ \mu M \leqslant [U]_{I_{AQ}} \leqslant 100\ \mu M$). Chisholm-Brause et al. (2001) have shown by TRLFS that four uranyl species coexist onto montmorillonite under certain conditions, with the preponderance of mononuclear, inner-sphere surface complexes at low (<3%) occupancy by U of surface sites, irrespective of aqueous monomeric or oligomeric U species ($3 \leqslant pH_F \leqslant 7$, $40\ \mu M \leqslant [U]_{I_{AQ}} \leqslant 200\ \mu M$). These studies show that the nature of U sorption species is function both of solution chemistry and of mineral surface characteristics.

Regarding Al-(hydr)oxides, two pH-dependent uranyl surface species have been observed by XPS and/or TRLFS at low U surface coverage ($\Gamma \leqslant 0.07$ μmol U/m^2) of γ-alumina (Kowal-Fouchard et al., 2004) and at moderate to high surface coverage ($0.05 \leqslant \Gamma \leqslant 0.5$ μmol U/m^2) of gibbsite (Baumann et al., 2005), for solids equilibrated with solutions at $[U]_{I_{AQ}}$ values of 100 and 10 μM, respectively. Baumann et al. (2005) have interpreted their results by the formation of polynuclear uranyl complexes at near-neutral pH in addition to the mononuclear inner-sphere complexation occurring at lower pH, based on the EXAFS study of Sylwester et al. (2000). Kowal-Fouchard et al. (2004) have suggested that the U surface species arise from the U aqueous speciation i.e. from the sorption of the free UO_2^{2+} ion at low pH, and of polynuclear species at pH > 5. Further work is however needed to assess the respective roles of aqueous species i.e. mononuclear vs. polynuclear species, and of surface parameters i.e. low vs. high U coverage, on the nature of the uranyl species onto Al-(hydr)oxides.

In this work, we aimed to identify surface species at low to moderate U surface coverage of amorphous Al-hydroxide, and to gain insights into their dependence on U solution species. Solid samples were obtained at a defined U loading ($\Gamma \approx 0.005$ or 0.05 μmol U/m^2) as a function of $[U]_{I_{AQ}}$ by adjusting in batch experiments the solid concentration of suspensions ($1\ g/L \leqslant C_{solid} \leqslant 100\ g/L$). We performed analyses of U sorbed at $pH_F \leqslant 5$ from solutions where either UO_2^{2+} ions or polynuclear/U(VI) colloids are expected to predominate ($[U]_{I_{AQ}} = 1$, 10, 50 or 100 μM). TRLFS was applied to detect distinct coordination environments of uranyl in the samples i.e. multiple U sorption species and/or emitting U components. EXAFS was used to provide the average of the chemical and structural environments of sorbed U and to complement the interpretation of TRLFS results in terms of U coordination environments.

2. Experimental and analytical section

2.1. Material and experiments

The chemicals used are of analytical grade (Merck). Attention was paid to minimize adsorbed carbonate species in sorption experiments (at $pH_F < 4.5$). Wijnja and Schulthess (1999) have evidenced no bands of adsorbed carbonates on the ATR-FTIR (Attenuated Total Reflectance Fourier Transform Infrared) spectra of aged γ-Al_2O_3 suspensions purged with pure air and at pH_F values of 4.5. We thus washed the initial γ-Al_2O_3 in N_2-atmosphere in order to remove autochthonous carbonate surface species prior to our experiments. All of the solution preparations and experiments were carried out in a glove box where a stream of N_2-gas was maintained, using CO_2-free NaOH/HCl solutions, ultra-pure water (resistivity: 18 MΩ) supplied directly from a Milli-Q apparatus, and bubbling of N_2-gas through initial solutions.

2.1.1. Solid pre-treatment

The initial γ-Al_2O_3 (Merck) was washed by pumping ultra-pure water through a series of filters containing solid sub-samples until the leachate resistivity is of ~18 MΩ (Froideval et al., 2003). The size fraction 63–100 μm of the sub-samples was collected and left for drying to constant weight (room temperature, N_2-atmosphere). The X-ray diffraction analysis of the dried solid indicated that γ-Al_2O_3 was completely transformed by leaching into an amorphous Al-hydroxide and into small amount of gibbsite indexed JCPDS 33-0018 and/or bayerite indexed JCPDS 20-0011. This is in agreement with studies showing the formation of bayerite and/or gibbsite in γ-alumina/solution systems at 298 K (Lefèvre et al., 2002; Kim et al., 2004). The specific surface area (S_A) of the dried sample is equal to 142 m^2/g.

2.1.2. Batch experiments of uranyl partitioning in Al-hydroxide/solution systems

Batch experiments were performed to measure at 298 K in N_2-atmosphere the partitioning of uranyl

between the mineral, colloidal and aqueous phases of Al-hydroxide/0.1 M $NaNO_3$ solution systems. The pH_F values were in the range 4–7. The parameter under investigation in a first series of experiments ($[U]_{I_{AQ}} \sim 50$ μM) was the concentration of solid (C_{solid}= 1, 5, 10, 25 or 50 g/L) i.e. of surface ligand ($[AlOH]_{S_{TOT}}$) in the system. The values of maximal U loading (Γ_{max}) were equal to ~0.350, ~0.070, ~0.035, ~0.014 or ~0.007 μmol U/m^2 solid, respectively. Experiments were also performed to evaluate the effect of $[U]_{I_{AQ}}$ ($[U]_{I_{AQ}} \approx 1$, 10 and 100 μM) at constant $[AlOH]_{S_{TOT}}/[U]_{I_{AQ}}$ values (i.e. at $\Gamma_{max} \approx 0.007$ and 0.07 μmol U/m^2 solid). A reference sample was made to measure the U uptake ($[U]_{I_{AQ}} \approx$ 1 mM) at pH_F of 3. The experimental procedure includes: (i) a 2-days period of shaking of the solid/electrolyte sample, (ii) a 3-days period of shaking of the U(VI)/solid/electrolyte sample (after initial pH adjustment and addition of a small volume of a $UO_2(NO_3)_2{\cdot}6H_2O$ solution in 10^{-2} M HNO_3) and (iii) a phase separation step as follows. The sample is centrifuged at 6000 rpm for 15 min. The supernatant is removed, filtered at 0.22 μm, and 5 ml of the filtrate is ultra-centrifuged at 50,000 rpm for 2 h for colloidal/aqueous phase separation. The ''mineral fraction'' collected after centrifugation i.e. the U-loaded Al-hydroxide and possibly uranyl precipitates, is left for drying to constant weight in the tube (298 K, N_2-atmosphere). The final pH is measured on both of the aliquots collected after centrifugation and filtration (which were found to display similar pH within the ΔpH_F error of 0.02). The final contents of dissolved U ($[U]_{F_{AQ}}$ in μM) and of total U in solution ($[U]_{F_{TOT,SOL}}$ in μM) i.e. dissolved and colloidal U species, were determined by ICP-MS analyses of the ultra-centrifuged and centrifuged solutions, respectively (error: 5%; detection limit: 0.1 ppb). The solutions were analysed for their final Al content by ICP-AES. The percents of total U removal from true solution (including colloids) and of U removal by sorption/precipitation are as follows:

$$\%\ \text{U removal (total)} = \left(\frac{\left([U]_{I_{AQ}} - [U]_{F_{AQ}}\right)}{[U]_{I_{AQ}}}\right) * 100 \qquad (1)$$

$$\%\ \text{U removal (sorption + precipitation)} = \left(\frac{\left([U]_{I_{AQ}} - [U]_{F_{TOT,SOL}}\right)}{[U]_{I_{AQ}}}\right) * 100$$

Blank experiments were performed using the same procedure as that described previously except that the Al-hydroxide was not added ($[U]_{I_{AQ}} = 1$, 10, 50 and 100 μM; $3 < pH_F < 7$; solution ageing time t_A: 15 min to 3 days). The experiments provided information on the stability of uranyl solutions i.e. on the formation of true U colloids and/or on the precipitation of uranyl oxide hydrates in CO_2-free U(VI)/0.1 $NaNO_3$ solution systems at 298 K.

2.2. Spectroscopic analyses

2.2.1. XAFS measurements

After drying to constant weight at 298 K in N_2-atmosphere (Section 2.1.2), the U-containing Al-hydroxide samples were removed from the experimental tubes. Subsamples were stacked into pellets, encapsulated between two Kapton foils and sealed with a polyethylene foil. A sub-sample of the synthetic meta-schoepite of Froideval et al. (2003) was used as a reference and was diluted in boron nitride before stacking. XAFS measurements were performed at the FAME beamline (BM 30B) at the European Synchrotron Radiation Facility (ESRF). Spectra were recorded at room temperature at the U L_3 edge, using a Si⟨220⟩ double monochromator. The calibration in energy was made using the first inflexion point of the L_3 edge of U metal (17166 eV). The meta-schoepite was analysed in transmission mode. The sorption samples were analysed in fluorescence mode, using a 30-elements solid state Ge detector (Canberra), with sample orientation of 45° to incident beam. Data reduction and analysis were performed using ifeffit and feffit softwares (Newville et al., 1995; Newville, 2001). Phase and amplitude were generated by the feff 8.1 code (Ankudinov and Rehr, 2000), for the model compounds α-$UO_2(OH)_2$ (Taylor and Hurst, 1971) and soddyite $(UO_2)_2SiO_4{\cdot}2H_2O$ (Demartin et al., 1992), in which Si atoms were replaced by Al atoms (Sylwester et al., 2000). All fitting operations were performed to Fourier transform (FT) spectra in R-space between 0.9 and 4.0 Å. The amplitude reduction factor S_0^2 was set to 1. The four-legged $U = O_{ax} = U = O'_{ax} = U$ path was used to model the trans-dioxo multiple scattering (MS) without adding variables to the fit, since its parameters were linked to those of the single scattering U–O_{ax} path, with N_{MS}, σ^2_{MS} and R_{MS} set, respectively, at $N_{MS} = N_{O_{ax}}$, $\sigma^2_{MS} = 2.\sigma^2_{O_{ax}}$, $R_{MS} = 2.R_{O_{ax}}$ (N: coordination number, σ^2: Debye–Waller factor, R: neighbour inter-atomic distance). For U–O_{eq} and U–U shells, the Debye–Waller factor and the coordination number were defined as free parameters during the fit and were found to be strongly correlated.

2.2.2. TRLFS measurements and analyses of fluorescence decay

Sub-samples of the dried U-containing Al-hydroxide solids and of the meta-schoepite were put in glass capillary tubes (optical quality, internal ∅: 2 mm, L: 5 cm). The tubes were tightly sealed before removal from the N_2-atmosphere glove box. The TRLFS measurements were performed at the Institut de Physique Nucléaire of Orsay and were collected on a system including a Continuum pulsed laser Nd:YAG (7 ns pulse duration) for sample excitation. The equipment is described by Kowal-Fouchard et al. (2004). The excitation wavelength was set to 430 nm. The fluorescence emission was measured in the range 470–600 nm. The uncertainties on the position of the uranyl emission bands were of ~1 nm. The fluorescence decay was measured within the interval time 0.1–2000 μs. The gate width was 2 μs.

The fluorescence intensity $F(\lambda, t)$, at wavelength λ and at time t, in presence of multiple emitting components j is described by

$$F(\lambda, t) = \sum_{j=1}^{n} F_j(\lambda, 0) \cdot \exp(-t/\tau_i) \quad (2)$$

where the pre-exponential factor $F_j(\lambda, 0)$ is the fluorescence intensity at time $t = 0$ of the emitting component j and τ_j is its lifetime.

The pre-exponential factor $F_j(\lambda, 0)$ depends on the experimental set-up (optical pathlength l, laser intensity I_0, factor k), on the molar absorption coefficient and on the fluorescence quantum yield of the component j, and on its concentration in sample. The values of $F_j(\lambda, 0)$ and of τ_j were obtained by a fitting procedure of the fluorescence decay curve (fluorescence intensity vs. time) using a third or a fourth-exponential function. The choice of the fitting function was based on considerations of residual and of reduced chi-square value (χ_r^2), as the goodness-of fit parameter, obtained using 1% error on experimental data points. Comparing the relative contributions p_i, associated to the pre-exponential factors a_i of the fitting function, is useful to evidence trends in concentration of the component i amongst related samples that are analysed and obtained under similar conditions. The relative contribution of a defined emitting component i, amongst the n emitting components j, to the overall fluorescence intensity is given by:

$$p_i = a_i.\tau_i / \sum_{j=1}^{n} a_j.\tau_j \quad (3)$$

The emission and the decay of fluorescence of the Al-hydroxide matrix were also measured. The matrix emitted a weak fluorescence signal and a bi-exponential decay function (lifetimes of ~9 and ~45 μs). The values of τ_i and of a_i for the matrix, were taken as fixed values in the fitting procedure used for sorption samples. The sum of the contributions p_i of the matrix to the fluorescence decay of the sorption samples was lower than 2%.

3. Results and discussion

3.1. Macroscopic uranyl uptake

Data of removal of aqueous U for 10^{-6}–10^{-4} M uranyl in CO_2-free, 0.1 M $NaNO_3$ solutions/suspensions of Al-hydroxide is reported in Fig. 1. Final solution concentrations

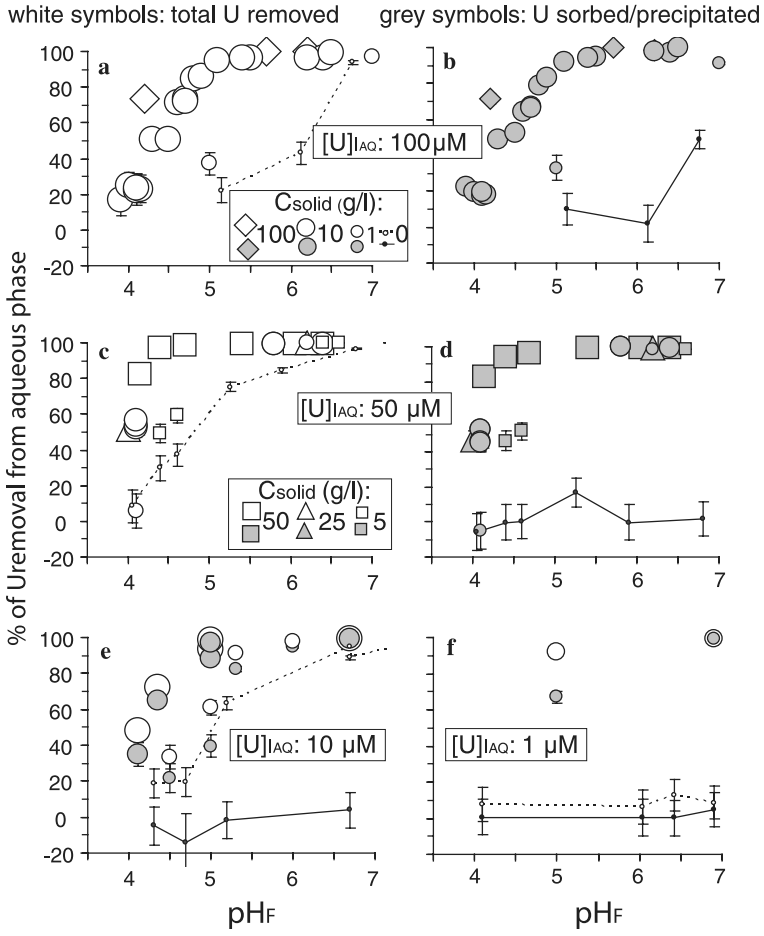

Fig. 1. Macroscopic uptake of aqueous uranyl in CO_2-free 0.1 M $NaNO_3$ solution/Al-hydroxide systems aged for 3 days, vs. final pH (pH_F). Effects of variable concentrations of initial aqueous uranyl, $[U]_{I_{AQ}}$, and of Al-hydroxide, C_{solid} (dashed and solid lines refer to total U removed and to U precipitated, respectively, in ageing solution experiments).

of U and Al, and related solubility curves, are given in electronic annex EA-1. Main results are as follows.

1. Solutions at $[U]_{I_{AQ}} \geqslant 10$ μM are unstable upon ageing and hydrolysis due to the formation of uranyl colloids (and of large particles at $[U]_{I_{AQ}} \approx 100$ μM and $pH_F \approx 7$). Final concentrations of aqueous uranyl ($[U]_{F_{AQ}}$) are close to equilibrium with respect to crystalline ($[U]_{I_{AQ}} \approx 10$μM) or meta-stable ($[U]_{I_{AQ}} > 10$ μM) uranyl oxide hydrates
2. Adding Al-hydroxide to the potentially unstable solutions suppresses the contribution of colloids to the removal of U from true solution. The uranyl removed is found in the mineral fraction. Its percentage increases with an increasing of the values of pH_F and of C_{solid} (at acidic pH_F). Values of $[U]_{F_{AQ}}$ in final solutions are below the predicted solubility of crystalline schoepite (except at $C_{solid} < 10$ g/L and $[U]_{I_{AQ}} \approx 100$ μM).
3. Adding Al-hydroxide to stable ~1 μM uranyl solutions leads to the removal of U by the mineral phase, >but generates U colloids at $pH_F \approx 5$. Sorption of U on Al-colloids, which are present at trace concentration level in the final solutions over-saturated with respect to gibbsite, may contribute to the percent of U removal at low $[U]_{I_{AQ}}$ values.

A major finding is the formation, within 3 days of reaction, of uranyl colloids in hydrolysed solutions at $[U]_{I_{AQ}} \geqslant 10$ μM, possibly as solubility-limiting schoepite or meta-stable schoepite-type phases, whose solubility constants are reported in Table 1. This agrees with studies showing the formation of U colloids in solutions where polynuclear aqueous U(VI) species pre-exist (Fig. 2) and of meta-stable uranyl oxide hydrates in super-saturated solutions (Dent et al., 1992; Torrero et al., 1994; Diaz-Arocas and Grambow, 1998). The major assessment of our experimental work is that sorption onto large surface areas of Al-hydroxide controls the removal of U from aqueous phase for such unstable solutions at $[U]_{I_{AQ}} \geqslant 10$ μM, as well as for the stable uranyl solutions. Such features are consistent with studies suggesting that aluminol groups at Al-oxide and clay surfaces act as strong ligands for U (McKinley et al., 1995; Turner et al., 1996; Del Nero et al., 1999; Wang et al., 2001). However, the question is, whether reactions at Al-hydroxide surface and reactions of formation of aqueous U oligomers/colloids compete amongst one another or cooperate to the sorption of uranyl. On the one hand, spectroscopic studies of Al-oxide and silica(te) surfaces have suggested the predominant role of U surface coverage over aqueous speciation on the formation of polynuclear uranyl surface species (Sylwester et al., 2000; Chisholm-Brause et al., 2001, 2004; Froideval et al., 2003; Froideval, 2004). On the other hand, it has been suggested that polynuclear U species on alumina arise from the adsorption of pre-existing solution species (Kowal-Fouchard et al., 2004). Speciation studies of U sorbed at low density on Al-hydroxide, in presence of mono- or polynuclear aqueous species, are crucial to assess the control exerted by abundant surface ligands vs. solution species on the U sorption species.

3.2. Presentation of the spectroscopic samples

TRLFS and EXAFS were applied to U-loaded Al-hydroxide samples obtained at $pH_F \leqslant 5$. Sorption samples at near-neutral pH, and a synthetic meta-schoepite (Froideval et al., 2003), were used as references. Spectroscopic sample conditions are listed in Table 2. The sample name relates to experimental conditions, as $[U]_{I_{AQ}}$–pH_F–C_{solid} ($[U]_{I_{AQ}}$ in μM, C_{solid} in g/L). Note that low U coverage samples were obtained over ranges of $[U]_{I_{AQ}}$ values (1–100 μM).

Table 1
Dissociation constants ($\log \beta^0_{p,q}$) for the aqueous phase and solubility constants of schoepite-type minerals ($\log K_{min}$) related to the reaction: $UO_3 \cdot 2H_2O_{(solid)} \leftrightarrow UO_2^{2+} + 3H_2O$ reported in the literature and used in this study

Species	$\log \beta^0_{p,q}$	Reference[a]
UO_2OH^+	−5.2	Grenthe et al. (1992)[a]
$UO_2(OH)_2$	−12.15	Guillaumont et al. (2003)
$UO_2(OH)_3^-$	−20.25	Guillaumont et al. (2003)
$(UO_2)_2(OH)_2^{2+}$	−5.62	Grenthe et al. (1992)[a]
$(UO_2)_3(OH)_5^+$	−15.55	Grenthe et al. (1992)[a]
$(UO_2)_3(OH)_7^-$	−32.20	Guillaumont et al. (2003)
$(UO_2)_4(OH)_7^+$	−21.9	Grenthe et al. (1992)[a]
$UO_2NO_3^+$	0.3	Grenthe et al. (1992)[a]
Schoepite mineral	$\log K_{min}$	**Reference**
Crystalline	4.83	Grenthe et al. (1992)[a]
Meta-schoepite	5.38	Torrero et al. (1994)
"Easily-forming"	5.37	Diaz-Arocas and Grambow (1998)
"Amorphous"	5.73	Torrero et al. (1994)

Values are at 298 K and at infinite dilution standard state.
[a] Value selected in the thermodynamic data compilation of Grenthe et al. (1992) and confirmed in the revised selection of Guillaumont et al. (2003).

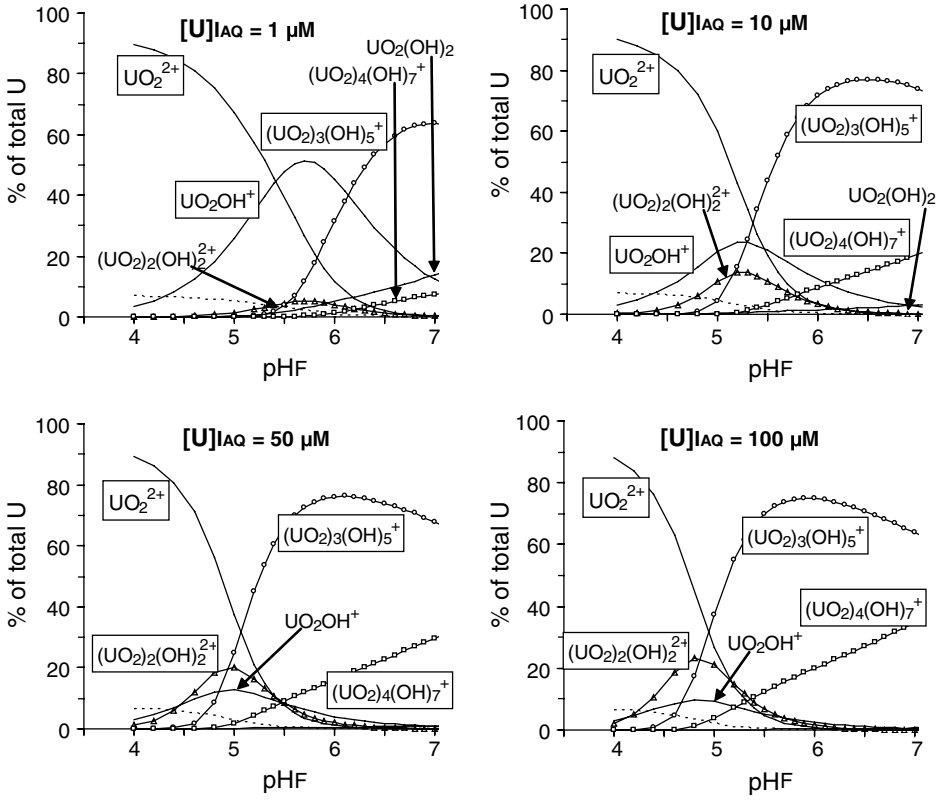

Fig. 2. Aqueous speciation diagrams, for different uranyl concentration levels ($[U]_{I_{AQ}}$) of CO_2-free 0.1 M $NaNO_3$ solutions at 298 K, calculated using data in Table 1. Solids are not allowed to precipitate (dashed line: $UO_2NO_3^+$ aqueous species).

Table 2
Experimental and spectroscopic conditions of U-containing Al-hydroxide sorption samples

Name and U loading, Γ, of the Al-hydroxide sorption samples and solid concentration, C_{solid}, of experiments				Experimental solutions: uranyl concentrations [U] in µM and final pH, pH_F			
Sample name $[U]_{I_{AQ}}$–pH_F–C_{solid}	C_{solid} (g/L)	U loading, Γ		pH_F	Initial U aqueous $[U]_{I_{AQ}}$	Final U total[a] $[U]_{F_{TOT,SOL}}$	Final U aqueous[a] $[U]_{F_{AQ}}$
		µmol U/g	µmol U/m^2				
1_5_1	1	0.5 ± 0.1	0.004 ± 0.001	5.0	1.26 ± 0.06	0.80 ± 0.04	0.10 ± 0.01
10_4.5_1	1	2.3 ± 0.9	0.02 ± 0.01	4.5	10.4 ± 0.5	8.1 ± 0.4	6.9 ± 0.3
50_4.4_5	5	5.0 ± 0.8	0.04 ± 0.01	4.4	54 ± 3	29 ± 2	27 ± 2
50_4.1_10	10	2.1 ± 0.3	0.02 ± 0.01	4.1	45 ± 2	25 ±1	20 ± 1
50_4.1_25	25	1.0 ± 0.2	0.007 ± 0.002	4.1	54 ± 3	28 ± 2	24 ± 1
50_4.2_50	50	0.9 ± 0.1	0.006 ± 0.001	4.2	54 ± 3	9.5 ± 0.5	9.3 ± 0.5
100_4.3_10	10	5.5 ± 0.8	0.04 ± 0.01	4.3	108 ± 5	54 ± 3	53 ± 3
100_4.2_100	100	0.9 ± 0.1	0.007 ± 0.002	4.2	124 ± 6	30 ± 2	28 ± 2
1000_3_100	100	5.8 ± 0.8	0.04 ± 0.01	3.0	960 ± 48	382 ± 19	383 ± 19
1_6.9_1	1	1.3 ± 0.2	0.009 ± 0.002	6.9	1.26 ± 0.06	0.01 ± 0.01	0.01 ± 0.01
50_6.2_1	1	52 ± 3	0.37 ± 0.02	6.2	53 ± 3	0.90 ± 0.06	0.10 ± 0.01

[a] cf. Section 1.1.2 and relation (1) in main text.

3.3. Average of surface structures on acidic-pH sorption samples

EXAFS spectroscopy is well suited to study the local structure of sorbed uranyl, i.e. element identities, distances and coordination numbers for atoms around the U atom, but the major limitation is that it observes the average of all surface structures present for adsorbing uranyl. The raw k^3-weighted EXAFS spectra of the sorption samples and of the meta-schoepite sample are shown in Fig. 3, along with the corresponding Fourier Transform (FT). The Fourier transformation yields a radial distribution of the near-neighbour atoms surrounding the U atom. The peaks on the FT spectra appear at shorter distances relative to the true neighbour distances (R) because of the electron scattering phase shifts ($\Delta R \sim 0.4$ Å). All the EXAFS spectra are dominated by the backscattering from the axial oxygen atoms (O_{ax}) of the linear UO_2^{2+} group (peak at 1.4 Å on the uncorrected FT). The second peak at ~2 Å on the FT is related to the backscattering from oxygen atoms in

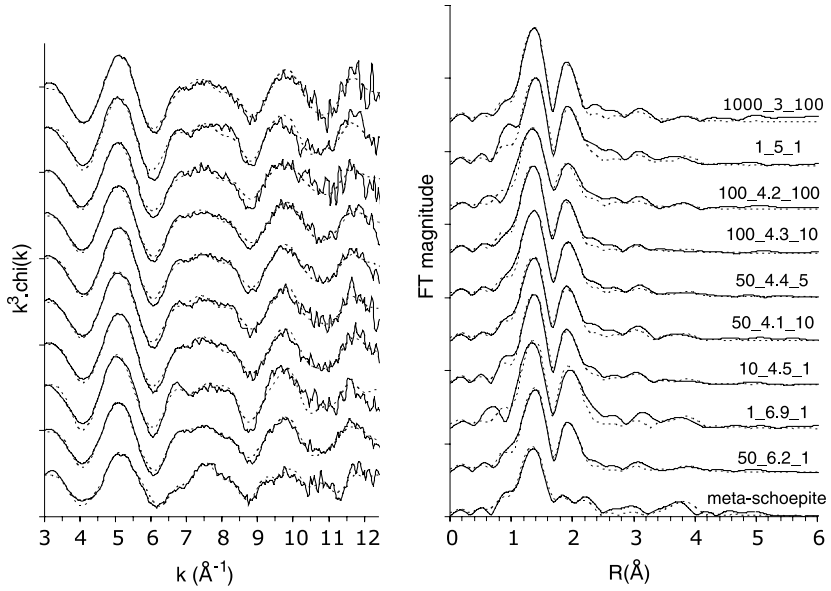

Fig. 3. Uranium L_3 EXAFS (left) and corresponding Fourier transform (right) for uranyl sorption samples and for the reference meta-schoepite (solid lines: experimental data; dashed lines: fits).

the equatorial plane (O_{eq}) of uranyl. The FT spectra show a peak at ~3 Å which corresponds to the multiple scattering effects of the U–O_{ax} coordination shell. The results of the data analyses are given in Table 3.

3.3.1. The acidic-pH sorption samples

The coordination environment of U is almost identical for all the sorption samples obtained at pH_F 4–5. The first coordination shell consists of the two axial oxygen atoms at a distance of 1.80 Å. The second shell is composed of 4–6 equatorial oxygen atoms at distances between 2.41 and 2.46 Å. For this shell, the coordination number and the Debye–Waller factor, taken as free parameters during the fits, are strongly correlated and the standard deviation on $N_{U-O_{eq}}$ values is estimated to be ±20%. The U–O_{eq} distances of 2.41–2.46 Å are close to those of U atoms coordinated by 5–6 equatorial oxygen atoms of aqueous species (Aberg, 1970; Dent et al., 1992; Chisholm-Brause et al., 1994; Allen et al., 1997; Thompson et al., 1997; Wahlgren et al., 1999) or of outer-sphere surface complexes onto clays (Chisholm-Brause et al., 1994; Hudson et al., 1999; Sylwester et al., 2000). They are also close to an average of the bond lengths reported for 5–6 oxygen atoms split in two equatorial subshells of sorbed U as a bidentate inner-sphere uranyl surface complex onto γ-alumina (Sylwester et al., 2000). The absence of equatorial splitting for our acidic-pH sorption samples may indicate outer-sphere surface complexes and/or multiple uranyl coordination environments (e.g. Elzinga et al., 2004). It may also result from the short *k*-range used in the measurements.

For all the sorption samples at pH_F 4–5, attributing the peak at ~3 Å on the uncorrected FT spectra to the multiple scattering effects of the U–O_{ax} shell provided a poor fit to the data. Several authors have reported that the peak feature at ~3 Å on FT spectra for uranyl onto several Al-silicates is the superposition of the multiple scattering (MS) effects of the U–O_{ax} shell and of the interactions between uranyl and substrate (Thompson et al., 1997; Hudson et al., 1999; Hennig et al., 2002). A significant fit improvement was obtained by adding in the data analyses the contribution of the single scattering originating from Al atoms of the Al-hydroxide. The procedure gives U–Al bond distances of ~3.38 Å and coordination numbers of 0.6–0.8 (± 20%). The presence of detectable U–Al interactions evidences that inner-sphere surface complexation is an important mechanism of adsorption of uranyl at acidic pH. The experimental U–Al bond length of ~3.38 Å matches the U–Al distance for the model structure of Hennig et al. (2002) with the uranyl unit ($R_{U-O_{eq}} = 2.35$ Å) in bidentate, edge-sharing connection with [AlO_6] octahedra ($1.85 < R_{Al-O} < 1.97$ Å). Assuming a monodentate surface complex would result in U–Al distances larger than the experimental ones (Hennig et al., 2002). The value of N_{U-Al} reported herein possibly results from multiple equatorial coordination environments i.e. ~70% ± 20% of the uranyl ions are bound to surface hydroxyls in a bidentate fashion and have one Al neighbour. For all the sorption samples at pH_F 4–5, a better fit was achieved (e.g. electronic annex EA-2) by including a U–U shell resulting in an average of one U neighbour (±20%) at 3.92 Å. Similar U–U distances are reported in the literature for aqueous polynuclear uranyl species (Aberg, 1970; Navaza et al., 1984; Dent et al., 1992; Moll et al., 2000) and for uranyl oxide hydrates (Allen et al., 1996). On the one hand, the EXAFS parameters give an average model structure consistent with a dinuclear, bidentate inner-sphere uranyl surface complex in edge-sharing connection with [AlO_6] octahedra. On the other hand, they are consistent with the existence of

Table 3
EXAFS parameters of U-containing Al-hydroxide sorption samples and of meta-schoepite

Sample name	Description of U coordination shells				E_0[b] (eV)	R-factor[c]
	U neighbour atom A_n	Coordination number[a] N_{U-A_n}	Interatomic distance[a] (Å) R_{U-A_n}	Debye–Waller factor[a] σ^2 (Å^2)		
1_5_1	O_{ax}	2[d]	1.81	0.003	0.5	0.07
	O_{eq}	4.7	2.46	0.009		
	Al	0.7	3.39	0.003[d]		
	U	1.0	3.92	0.006		
10_4.5_1	O_{ax}	2[a]	1.80	0.003	−1.2	0.03
	O_{eq}	4.5	2.43	0.010		
	Al	0.7	3.36	0.003[d]		
	U	1.2	3.93	0.010		
50_4.4_5	O_{ax}	2[d]	1.80	0.003	−0.9	0.03
	O_{eq}	4.3	2.43	0.009		
	Al	0.7	3.39	0.003[d]		
	U	1.4	3.94	0.011		
50_4.1_10	O_{ax}	2[d]	1.80	0.004	−2.9	0.03
	O_{eq}	4.1	2.42	0.009		
	Al	0.7	3.36	0.003[d]		
	U	0.9	3.93	0.006		
100_4.3_10	O_{ax}	2[d]	1.79	0.003	−4.1	0.02
	O_{eq}	4.5	2.41	0.010		
	Al	0.4	3.38	0.003[d]		
	U	1.1	3.91	0.012		
100_4.2_100	O_{ax}	2[d]	1.79	0.004	−4.4	0.05
	O_{eq}	5.6	2.41	0.013		
	Al	0.8	3.39	0.003[d]		
	U	1.1	3.90	0.009		
1000_3_100	O_{ax}	2[d]	1.80	0.003	−1.9	0.003
	O_{eq}	3.6	2.41	0.007		
	Al	0.8	3.39	0.003[d]		
	(U)	(0.5)	(3.92)	(0.006)		
50_6.2_1	O_{ax}	2[d]	1.81	0.003	−0.4	0.02
	O_{eq}	3.5	2.43	0.008		
	U	1.8	3.93	0.012		
1_6.9_1	O_{ax}	2[d]	1.80	0.003	−0.7	0.06
	O_{eq}	4.7	2.45	0.008		
	U	1.2	3.93	0.005		
Meta-Schoepite	O_{ax}	2[d]	1.79	0.005	−1.1	0.05
	O_{eq1}	1.9	2.32	0.009		
	O_{eq2}	1.8	2.51	0.006		
	U	1.9	3.91	0.007		

[a] $\Delta N_{U-A_n} = 20\%$; $\Delta R_{U-A_n} = 0.02$ Å; $\Delta\sigma^2 = 0.001$–0.002 Å^2.
[b] Shift in threshold energy.
[c] Goodness of fit defined as the weighted sum of squares of residuals divided by the degree of freedom.
[d] Held constant during the fit.

multiple U species, e.g. inner-sphere surface complexes as mononuclear and/or dinuclear species, polynuclear surface oligomers/surface precipitates and possibly outer-sphere complexes. The reference samples presented hereafter provide examples of species possibly coexisting on Al-hydroxide at pH_F 4–5. The present EXAFS study indicates that inner-sphere surface complex formation, and (surface) polynucleation, are major mechanisms competing against U colloid formation at acidic pH. Highly-reactive, singly-coordinated terminal hydroxyl groups (Bargar et al., 1997), at surfaces of gibbsite/bayerite present in small amount in the Al-hydroxide phase used, may partly account for the high surface affinity of the phase towards uranyl.

3.3.2. EXAFS results for the reference sample 1000_3_100

The difference between the reference sample 1000_3_100 obtained at pH_F 3 and the sorption samples at pH_F 4–5 is evident in the U–U coordination shell. Introducing a U–U shell for the sample 1000_3_100 leads to no significant fit improvement. When assuming U–U interactions, the fitting procedure gives ~0.4 near-neighbour U atoms. Thus, no (or only a few) polynuclear uranyl species occur in this sample. The sorption of U(VI) at pH_F 3 on Al-hydroxide results in predominant mononuclear surface species, with $80\% \pm 20\%$ of the uranyl ions sorbed through inner-sphere complexation in a bidentate fashion. This is in a good agreement with previous EXAFS data on the sorption of U at pH 3–4 on

(hydr)oxides (Waite et al., 1994; Reich et al., 1996, 1998; Moyes et al., 2000; Sylwester et al., 2000).

3.3.3. EXAFS results for the reference sample 50_6.2_1 and for the meta-schoepite

Unlike for the acidic-pH sorption samples, no Al shell was detected in the sample 50_6.2_1 obtained at near-neutral pH_F and at high U loading. Uranyl is found surrounded by ~4 equatorial oxygen atoms at a mean distance of 2.43 Å and by ~2 (±20%) uranium atoms at 3.93 Å. Such a structure resembles that of the meta-schoepite sample except that the O_{eq} atoms in meta-schoepite are split in two sub-shells, as reported by Allen et al. (1996). Uranyl probably occurs as poorly crystalline U(VI) oxide hydrates in the sample 50_6.2_1. The precipitation of large particles out of the highly over-saturated initial solution might be favoured by the low concentration of solid used in the experiment. The retention of U colloids on Al-hydroxide can not be ruled out, because true U colloids are abundantly formed upon aging of hydrolysed solutions at $[U]_{I_{AQ}} \approx 50$ μM (Fig. 1). This sample is thus representative of poorly crystalline uranyl oxide hydrates forming under our experimental conditions.

3.3.4. EXAFS results for the reference sample 1_6.9_1

Uranyl oxide hydrate precipitates and/or colloids are unlikely to contribute significantly to sorbed uranyl in the high surface coverage sample 1_6.9_1 obtained at near-neutral pH_F, because the solution at $[U]_{I_{AQ}} \approx 1$ μM used in the experiment is stable (Fig. 1). On the one hand, the mean structural parameters of the U–O_{eq} shell and of the U–U shell ($N_{U-U} = 1.2 \pm 0.3$; $R_{U-U} = 3.93$ Å) are close to those of the sorption samples at pH_F 4–5. On the other hand, no Al shell is present at 3.38 Å. At high sorption density, uranyl ions form predominantly polynuclear surface oligomers and/or amorphous surface precipitates on the Al-hydroxide brought in contact with stable and near-neutral uranyl solutions.

3.4. TRLFS evidences for multiple U components in the acidic-pH sorption samples

Spectra of the emission of fluorescence of uranyl species/compounds have a great variability in spite of characteristic resolved vibronic structures. They are sensitive to environmental sample parameters (e.g. hydration) and to molecular structural factors such as solvation and bonding modalities in the equatorial plane of the uranyl moiety. Also the decay of the fluorescence emission for uranyl in a species/compound is related to its coordination environment (as well as to environmental and intrinsic electronic factors). Different bonding environments may thus shift the peak positions and/or lifetime values. For example, lifetimes larger than that of aqueous UO_2^{2+} ions have been reported for hydrolysis species (e.g. Kato et al., 1994; Moulin et al., 1995, 1998; Eliet et al., 2000; Kirishima et al., 2004) and for inner-sphere surface complexes (Gabriel et al., 2001; Chisholm-Brause et al., 2001; Chisholm-Brause et al., 2004; Kowal-Fouchard et al., 2004; Walter et al., 2005), due to replacements of H_2O ligands of the aquo uranyl ion by OH^- ligands or surface hydroxyls, respectively. TRLFS is a powerful tool to detect distinct surface coordination environments of U i.e. multiple U surface "components". Major limitations concern the assignment of the emission characteristics to surface species. No relationships exist to describe the fluorescence properties of the U surface species as a function of their structure and composition, or of sample parameters. Moreover, lifetimes are sensitive to non-equivalent U atoms possibly coexisting in a single surface species, as claimed by Catalano and Brown (2005). Providing references internal to the system under study for the fluorescence emission characteristics is thus useful for surface species identification.

3.4.1. TRLFS results for the acidic-pH sorption samples

Fluorescence emission spectra- The fluorescence emission spectrum of U sorbed at pH_F 3 (sample 1000_3_100) is well resolved and is characterized by peak maxima at 498, 519 and 540.5 nm (Fig. 4 and Table 4). These values are close to those reported for envelope spectra of sorbed uranyl species (Table 5). The spectra of our samples at $pH_F \leqslant 5$ show no marked variation in the shape and position of the peaks as function of the values of Γ or $[U]_{I_{AQ}}$, and are almost similar to that of the sample 1000_3_100 (Fig. 4). Thus, emitting U components may be of similar nature for all the sorption samples. There just observes a small change in the peak intensities ratio with an increasing of the Γ value, which suggests multiple U(VI) components whose relative proportion depends on U loading.

Lifetime measurements. The fluorescence decay experiments strongly support multiple emitting uranyl components i.e. U atoms in distinct coordination environments. Fitting analyses indicate at least three components of distinct lifetimes (Fig. 5a). Assuming a fourth-exponential function for fitting decay curves provides reasonable values of the goodness-of-fit parameter (χ_r^2) and lifetime values from short ($\tau_1 = 9 \pm 3$ and $\tau_2 = 31 \pm 10$) to long ($\tau_3 = 85 \pm 25$ and $\tau_4 = 210 \pm 40$). Similar lifetime values are resolved for all the sorption samples at $pH_F \leqslant 5$ (Fig. 5b). Trends in the relative contribution of component i to the decay for these related samples, i.e. in percentage p_i (relation 3), provides information on trends in the concentration of the component i. The p_i values for the sample 1000_3_100 indicate a major contribution of longer-lived components to fluorescence decay (Table 4). The percentages p_i for all the acidic sorption samples fall within the large error bars associated to suchp_i values. So, fluorescence data of U sorbed on Al-hydroxide indicate multiple emitting U components of distinct lifetimes, similar in nature and possibly close in distribution for all the sorption samples at $pH_F \leqslant 5$, despite different U surface coverage and aqueous U concentrations.

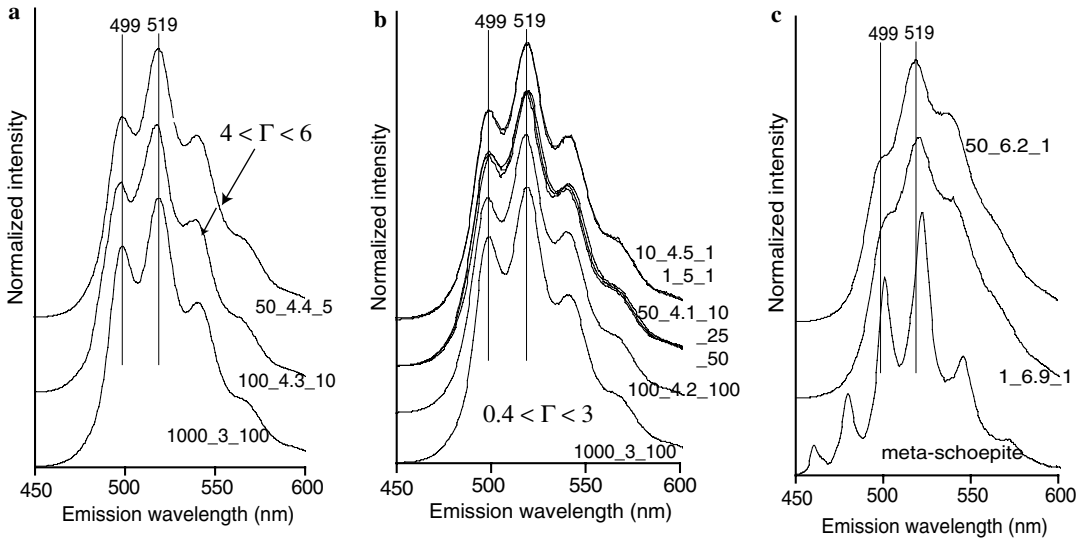

Fig. 4. Fluorescence emission spectra of uranyl sorption samples obtained (a) and (b) at acidic pH and at different U loadings (Γ in μmol U/g solid) and (c) at near-neutral pH. The spectra of 1000_3_100 and of meta-schoepite are reported in (ab) and (c), respectively.

Table 4
Fluorescence characteristics of reference samples: main emission bands and fit results of decay data

Sample name $[U]_{I_{AQ}}\_pH_F\_C_{solid}$	Fluorescence decay parameters[a] (fit): lifetime τ_i (μs), percentage p_i (%) and goodness-of fit χ_r^2					Fluorescence emission line width (description) and main bands (nm)
	τ_1 (p_1)	τ_2 (p_2)	τ_3 (p_3)	τ_4 (p_4)	χ_r^2	
1000_3_100	16 ± 2 (14 ± 4)	48 ± 4 (22 ± 6)	116 ± 9 (49 ± 13)	247 ± 25 (15 ± 9)	1.4	Structured 498; 519; 541
1_6.9_1[b]	18 ± 2 (15 ± 5)	49 ± 6 (30 ± 10)	106 ± 12 (37 ± 12)	233 ± 15 (18 ± 9)	2.5	Broad, centered at 521 Shoulder at 535–540
50_6.2_1[c]	11 ± 1 (36 ± 5)	40 ± 2 (45 ± 8)	141 ± 6 (17 ± 7)		0.6	Broad, centered at 519 Shoulder at 532–540
Meta-schoepite	11 ± 2 (22 ± 7)	41 ± 3 (52 ± 15)	134 ± 7 (26 ± 10)		0.7	Structured 460; 480; 500; 521; 545; 572

[a] cf. Section 1.2.2 of main text.
[b] Assuming three exponentials in the fit suppresses the contribution of τ_1.
[c] Assuming four exponentials in the fit leads to $p_4 \leqslant 10\%$ and does not improve value of χ_r^2.

3.4.2. Comparison with the meta-schoepite reference and literature data

TRLFS results for the meta-schoepite reference sample. The well-resolved spectrum of meta-schoepite exhibits six fluorescence maxima and a main peak at 522 nm (Table 4). TRLFS studies of schoepite have reported structureless or broad spectra at 523–535 nm (Table 6). The structure of meta-schoepite consists of layers of stoichiometry $(UO_2)_4O(OH)_6$, formed from edge-sharing UO_7 pentagonal bipyramids, with five O_{eq} atoms split in five U–O_{eq} shells at distances between 2.18 and 2.63 Å and four non-equivalent U atoms having slightly different U–O_{eq} values (Weller et al., 2000). All the U atoms of the meta-schoepite reference sample appear identical when analysed by XPS (Froideval et al., 2003) or by EXAFS, which gives a single U atom having ~4 O_{eq} split in two equatorial shells (Table 3). By contrast, three uranyl components are resolved from the meta-schoepite fluorescence decay which is dominated by the contribution of the short-lived components τ_1 and τ_2 (Table 4). This does not mean that lifetime analysis allows identifying all non-equivalent U atoms in the meta-schoepite. Several authors have reported, for schoepite-like phases, a single lifetime whose value may depend on phase crystallization (Table 6). Moreover, other factors such as sample hydration induce shifts in lifetime values. The sample presented here is made up of meta-schoepite and dehydrated schoepite (Froideval et al., 2003), which may contribute to the different lifetime components.

Comparison with the acidic-pH sorption samples. The meta-schoepite exhibits short lifetime values (τ_1 and τ_2) and a lifetime value τ_3 comparable to those of the sorption samples. Such a finding is not an evidence of the existence of meta-schoepite and/or schoepitic precipitates in the sorption samples. Very short to long lifetimes have been resolved for emitting uranyl complexes onto Al-(hydr)oxides and montmorillonite, and have tentatively been assigned by authors to different uranyl surface species (Table 5). Moreover, aqueous uranyl hydrolysis species display life-

Table 5
Fluorescence data (emission bands and lifetimes τ_i), and authors assignment, of uranyl species sorbed on Al-(hydr)oxides and montmorillonite under different experimental conditions

Sorbent	Conditions	Fluorescence		Main emission peaks[d] (nm)	Reference
	$[U]_{I_{AQ}}$ (μM); pH_F; Γ (μmol/g)	τ_i[b] ($\Delta\tau_i$) (μs)	Species assignment[c]		
Gibbsite	~9; 5; 1	122	Mo IS SC	502–526 unst.	Chisholm-Brause et al. (2004)
	~9; 8; 17	120	Po IS SC	510–529 unst.	
Gibbsite S_A[a]: 1.5	10; 5–8; ~0.1–0.8	0.33	Mo IS SC	~497, 519, 541	Baumann et al. (2005)[f]
		5.6	Po IS SC		
γ-Alumina S_A[a]: 140	100; 4.3; ~6	45 (5)	Mo IS SC	498, 518, 540	Kowal-Fouchard et al. (2004)
	100; 6.3; ~10	45(5)	Mo IS SC	497, 518, 540	
		120(10)	Po IS SC		
Montmorillonite CEC[a]: 1.2	~40; 3.5–5.8; 1.4–2.0	2–12	OS SC	~500, 519, 540	Chisholm-Brause et al. (2001)
		170–270	Mo IS SC		
	~1000; 3.5–5.8; 34–52	170–270	Mo IS SC	~497, 519, 541[e]	
		15–25	Pm SC	To unst.	

[a] S_A specific surface area (m^2/g); CEC: cation exchange capacity (meq/g).
[b] Values reported when given by authors.
[c] Mo, mononuclear; Po, polynuclear; Pm, polymeric; IS, inner-sphere; OS, outer-sphere; SC, surface complex.
[d] "envelope" spectrum if multiple sorption species occur; unst., unstructured spectrum.
[e] An unstructured time-resolved spectrum (centered at ~521 nm) is given by authors for Pm SC.
[f] Measurements were performed for gibbsite suspensions.

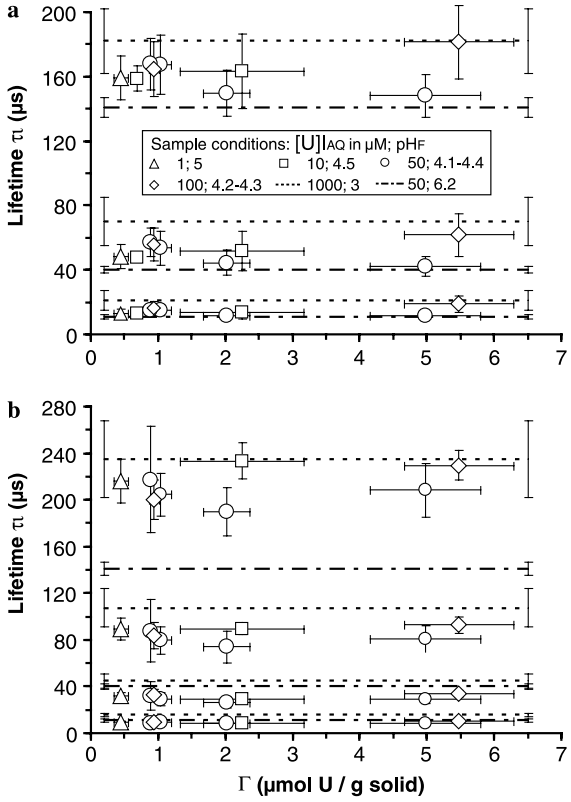

Fig. 5. Lifetime values, τ_i, of emitting uranyl components obtained by using (a) third-exponential or (b) fourth-exponential functions in fitting fluorescence decay, vs. U loading, Γ, of sorption samples obtained at different initial aqueous U concentration ($[U]_{I_{AQ}}$) and final pH (pH_F). Dotted and dashed-dotted lines refer to the references 1000_3_100 and 50_6.2_1, respectively

time values between 10 and 33 μs (Table 6). Thus, the assignment of the emitting U components of lifetimes τ_1, τ_2 and τ_3 in the acidic sorption samples, cannot be made on basis of lifetime measurements for non-related samples.

3.4.3. Comparison with the related samples 50_6.2_1 and 1_6.9_1

It is useful to compare the fluorescence characteristics of the sorption samples to those of the U(VI) oxide hydrates and surface oligomers forming under our experimental conditions. The emission spectra of uranyl sorbed at moderate/high surface coverage show a marked variation with a drop of pH_F from acidic to near-neutral (Fig. 4), regardless of the initial aqueous uranyl concentration ($[U]_{I_{AQ}} \approx 1$ μM or ≈50 μM). Unlike for the acidic-pH sorption samples, the spectra of the samples 50_6.2_1 and 1_6.9_1 are unresolved and display one fluorescence maximum centered at 519–521 nm. However, polynuclear surface oligomers/amorphous surface precipitates (sample 1_6.9_1) exhibit fluorescence decay features close to those of acidic-pH sorption samples (Table 4). A long lifetime of ~200 μs (τ_4) is resolved, when using either a fourth- or a third-exponential fitting function (cf. footnotes in Table 4). By contrast, the contribution of τ_4 to the fluorescence decay of amorphous uranyl oxide hydrates (sample

Table 6
Fluorescence data (emission bands and lifetimes τ_i) of aqueous uranyl species and of U(VI) oxide hydrates reported in the literature

Aqueous species/U(VI) oxide hydrate	$\tau_i \pm \Delta t_i$[a] (μs)	Emission band (nm) Line width (description)	Reference
UO_2^{2+}	2.3 ± 0.4	Narrow, 488, 510, 533	Kirishima et al. (2004)
UO_2OH^+	11.3 ± 4.5	Narrow, 497, 519, 543	
$(UO_2)_2(OH)_2^{2+}$	17.8 ± 2.8	Broad, 498, 515, 534	
$(UO_2)_3(OH)_5^+$	33.3 ± 5.2	Broad, 498, 514, 535	
Uranyl hydroxide solids	63 ± n.r.[b]	Unstructured	Chisholm-Brause et al. (2001)
	131 ± n.r.[c]	Unstructured	
	n.r.[b]	Unstructured, 549–559	Morris et al. (1996)
Schoepite minerals	n.r	Unstructured, centered at ~529	
	n.r.	Unstructured, 523–533	

[a] n.r.: not reported by authors.
[b] Fresh precipitate.
[c] Aged precipitate.

50_6.2_1) is not firmly established (cf. footnotes in Table 4). Three components of lifetimes τ_1, τ_2 and τ_3 are univocally resolved for this sample and the shorter-lived ones mainly contribute to the fluorescence decay. Such findings are of importance because they strongly support that the longer-lived emitting component (τ_4) is related to U binding at surface groups i.e. to replacement of H_2O ligands of aquo UO_2^{2+} ions by surface hydroxyl groups.

3.5. Discussion: single sorption species versus multiple sorption species

The reference sample 1000_3_100 having U atoms in mononuclear, bidentate inner-sphere surface complexes are characterized by the presence of the long lifetime τ_4 and by the preponderant contribution of long-lived components (τ_3 and τ_4) to its fluorescence decay, unlike the amorphous uranyl oxide hydrates (sample 50_6.2_1). We thus attribute the component(s) of lifetime of 170–260 μs present in all the sorption samples at pH_F 4–5 (and in the sample 1_6.9_1 made up by polynuclear surface oligomers) to "surface U atoms" i.e. to U atoms directly bound to surface hydroxyl groups. Similarly, the lifetime τ_3 of these samples is tentatively attributed to inner-sphere surface complexes/species because it dominates their fluorescence decay (unlike for sample 50_6.2_1).

Assigning components of lifetimes τ_3 and τ_4 to precise U coordination environments is difficult. Because the influence of near-neighbour U atoms on fluorescence properties of surface U atoms is unknown, the range of lifetime 170–260 μs may relate to surface U atom(s) in mononuclear surface complexes and/or in polynuclear surface oligomers. Similarly, the lifetime τ_3 may relate either to surface U atoms or to U atoms of dinuclear surface complexes/polynuclear surface oligomers not directly anchored to aluminol sites. Baumann et al. (2005) have argued, since H_2O in the coordination environment of uranyl quenches fluorescence lifetime, that clusters of polynuclear surface species have lifetimes larger than that of mononuclear, bidentate inner-sphere complex on aluminol groups of gibbsite. By contrast, Chisholm-Brause et al. (2001) have suggested that loss of coordinated water of inner-sphere U(VI) sorption complexes (relative to aqueous uranyl species) results in long fluorescence lifetimes, whereas polymeric surface species on montmorillonite exhibit shorter lifetimes as poorly crystalline phases. In the present state of knowledge, it is not possible to extract precise structural information from uranyl lifetimes in complex sorption systems. Further TRLFS analyses on reference samples are needed to determine the effects on uranyl fluorescence properties of loss of hydration water molecules in inner-sphere surface complex, of different U coordination environments in polymeric surface species, and of crystallinity of U(VI) hydroxide-like phases. So the absolute lifetime values of the longer-lived components provide no clear insights into the occurrence of mononuclear vs. dinuclear surface complex in samples at pH_F 4–5. Only the similarity between the emission spectra of all the acidic-pH sorption samples (including 1000_3_100) suggests the persistence of mononuclear, inner-sphere U surface complexes onto Al-hydroxide, when increasing the pH from 3 to 5.

By contrast, the lifetime measurements strongly support the existence of U emitting components similar to those in amorphous uranyl oxide hydrates, and in polynuclear surface oligomers/amorphous surface precipitates, for all the Al-hydroxide samples brought in contact with diluted or concentrated uranyl solutions at acidic pH. Indeed, the presence of the four fluorescent U components in these samples, including those characteristics of the amorphous uranyl oxide hydrates (τ_1 and τ_2), disagrees with the interpretation of the EXAFS data as a single dinuclear, bidentate inner-sphere surface complex. Such a complex displays two kinds of U atoms i.e. the surface U atom and its neighbour U atom, provided all sorption sites are similar. Even in the case of multiple sites inducing shifts in lifetime, it is unlikely that U in dinuclear, bidentate inner-sphere surface complexes display lifetimes similar to those (τ_1 and τ_2) which dominate the fluorescence decay of distinct schoepitic phases (the meta-schoepite and the amorphous uranyl oxide hydrates).

Thus, we interpret the fractional coordination number N_{U-Al} recorded by EXAFS for the sorption samples at pH_F 4–5 as multiple sorption species i.e. as predominant inner-sphere mononuclear and dinuclear surface complexes,

and as additional surface species having U in uranyl (hydr)oxide-type coordination environment. Because large particles of schoepite precipitating out from solution are unlikely at pH 4–5, these surface species may result (i) from the retention of uranyl colloids existing in solution, and/or (ii) from the surface polymerization/surface precipitation of uranyl ions. Finally, both the EXAFS and fluorescence lifetime measurements are also consistent with the contribution of outer-sphere surface complexes of aqueous uranyl hydrolysis species of short lifetimes (Table 6), for all sorption samples at pH_F 4–5. The contribution of such species is expected to be low, because they occur as minor aqueous species under such pH conditions (Fig. 2).

4. Conclusions

This work is a valuable contribution towards a better understanding of the respective roles of the solution and surface parameters which control the uptake of U by hydroxides. A major finding is that uranyl is mainly sorbed, at pH < 5, through mechanisms of inner-sphere surface complex formation on large surface areas of Al-hydroxide, irrespective of preponderant monomeric or oligomeric (potentially colloidal) uranyl species of initial solutions. Thus, high-affinity surface aluminol sites strongly control the nature of the uranyl species formed at low/moderate sorption density on Al-hydroxide.

Another important finding is that multiple uranyl sorption complexes co-exist at low coverage by U of the Al-hydroxide surface. Whereas the U surface speciation at pH 3 is dominated by a mononuclear, inner-sphere uranyl surface complex, the EXAFS data indicate a dinuclear, bidentate, inner-sphere uranyl surface complex as an average of surface structures at pH 4–5. The TRLFS data complement such structural information and evidence that the uranyl surface speciation is complex. Sorbed U appears in the form of mononuclear and/or dinuclear inner-sphere surface complexes, and of minor surface species with U atoms in coordination environments close to those of uranyl oxide hydrates, even for stable initial U solutions. The minor surface species may thus result from polymerization/surface precipitation of uranyl ions. Such a result stresses again the important role of the surface characteristics of Al-phases (abundance of strong sites, surface structure) on the uranyl surface speciation. In the case of potentially highly unstable solutions, one cannot rule out that small amounts of U colloids are formed, despite inner-sphere surface complexation, and are sorbed on the Al-hydroxide.

The results presented herein are of interest for the transport of uranyl in subsurface systems characterized by moderately acidic and poorly carbonated solutions. They suggest that surfaces of amorphous Al-hydroxide retard the migration of U in stable and poorly concentrated uranyl solutions via continuous processes, from the formation of mononuclear bidentate, inner-sphere surface complex to the surface polymerization. Moreover, large surface areas of Al-hydroxide in contact with unstable, acidic uranyl solutions may also prevent the migration of schoepite-type colloids (i) by the formation of inner-sphere surface complexes competing to a large extent against the formation of U colloids, (ii) and by sorption of the uranyl colloids formed in small quantities.

Acknowledgments

The authors gratefully acknowledge the Associate Editor Prof. W. Casey, and three anonymous reviewers for their critical comments and for manuscript improvement. We thank J. Samuel from the Centre de Geochimie de la Surface (CGS) of Strasbourg (France) for ICP-MS measurements and G. Lagarde from the Institut de Physique Nucléaire of Orsay for his technical support for TRLFS analyses. We gratefully acknowledge the staff members of the FAME beamline of the European Synchrotron Radiation Facility (ESRF) of Grenoble (France) for their technical assistance.

Associate editor: William H. Casey

Supplementary material

Supplementary data associated with this article can be found, in the online version, at doi:10.1016/j.gca.2006.08.027.

References

Aberg, M., 1970. On the structures of the predominant hydrolysis products of uranyl (VI) in solution. *Acta Chem. Scand.* **24**, 2901–2915.

Allen, P.G., Shuh, D.K., Bucher, J.J., Edelstein, N.M., Palmer, C.E.A., Silva, R.J., Nguyen, S.N., Marquez, L.N., Hudson, E.A., 1996. Determinations of uranium structures by EXAFS: schoepite and other U(VI) oxide precipitates. *Radiochim. Acta* **75**, 47–53.

Allen, P.G., Bucher, J.J., Shuh, D.K., Edelstein, N.M., Reich, T., 1997. Investigations of aquo and chloro complexes of UO_2^{2+}, NpO_2^{+}, Np^{4+} and Pu^{3+} by extended X-ray absorption fine structure spectroscopy. *Inorg. Chem.* **36** (21), 4676–4683.

Ankudinov, A., Rehr, J.J., 2000. Theory of solid-state contributions to the X-ray elastic scattering amplitude. *Phys. Rev. B* **62**, 2437–2445.

Arnold, T., Zorn, T., Bernhardt, G., Nitsche, H., 1998. Uranium(VI) sorption onto phyllite. *Chem. Geol.* **151**, 129–141.

Bargar, J.R., Towle, S.N., Brown Jr., G.E., Parks, G.A., 1997. XAFS and bond valence determination of the structures and compositions of surface functional groups and Pb(II) and Co(II) sorption products on single crystal α-Al_2O_3. *J. Colloid Interf. Sci.* **186**, 473–492.

Bargar, J.R., Reitmeyer, R., Lenhart, J.J., Davis, J.A., 2000. Characterization of U(VI) – carbonato ternary complexes on hematite: EXAFS and electrophoretic mobility measurements. *Geochim. Cosmochim. Acta* **64**, 2737–2749.

Baumann, N., Brendler, V., Arnold, T., Geipel, G., Bernhard, G., 2005. Uranyl sorption onto gibbsite studied by time-resolved laser-induced fluorescence spectroscopy (TRLFS). *J. Colloid Interf. Sci.* **290**, 318–324.

Bruno, J., Duro, L., de Pablo, J., Casas, I., Ayora, C., Delgado, J., Gimeno, M.J., Peña, J., Linklater, C., Pérez del Villar, L., Gomez, P., 1998. Estimation of the concentrations of trace metals in natural systems. The application of codissolution and coprecipitation approaches to El Berrocal (Spain) and Poços de Caldas (Brazil). *Chem. Geol.* **151**, 277–291.

Bruno, J., Duro, L., Grivé, M., 2002. The applicability of thermodynamic geochemical models to simulate trace element behaviour in natural waters. Lessons learned from natural analogue studies. *Chem. Geol.* **190**, 1–4 (see also pp. 371–393).

Catalano, J.G., Brown Jr., G.E., 2005. Uranyl adsorption onto montmorillonite: evaluation of binding sites and carbonate complexation. *Geochim. Cosmochim. Acta* **69** (12), 2995–3005.

Chisholm-Brause, C.J., Conradson, S.D., Buscher, C.T., Eller, P.G., Morris, D.E., 1994. Speciation of uranyl sorbed at multiple binding sites on montmorillonite. *Geochim. Cosmochim. Acta* **58** (17), 3625–3631.

Chisholm-Brause, C.J., Berg, J.M., Matzner, R.A., Morris, D.E., 2001. Uranium(VI) sorption on montmorillonite as a function of solution chemistry. *J. Colloid Interf. Sci.* **233**, 38–49.

Chisholm-Brause, C.J., Berg, J.M., Little, K.M., Matzner, R.A., Morris, D.E., 2004. Uranyl sorption by smectites: spectroscopic assessment of thermodynamic modeling. *J. Colloid. Interf. Sci.* **277** (2), 366–382.

Del Nero, M., Salah, S., Miura, T., Clément, A., Gauthier-Lafaye, F., 1999. Sorption/desorption processes of uranium in clayey samples of the Bangombé natural reactor zone. *Gabon. Radiochim. Acta* **87**, 135–149.

Del Nero, M., Froideval, A., Gaillard, C., Mignot, G., Barillon, R., Munier, I., Ozgümüs, A., 2004. Mechanisms of uranyl sorption. In: Gieré, R., Stille, P. (Eds.), *Energy, Waste and the Environment: A Geochemical Perspective, Chapter IV: Waste-Waste Interaction. Geological Society Special Publication 236*. Geological Society, London, UK, pp. 545–560.

Demartin, F., Gramaccioli, C.M., Pilati, T., 1992. The importance of accurate crystal structure determination of uranium minerals. II. Soddyite $(UO_2)_2(SiO_4)\cdot 2H_2O$. *Acta Cryst. C* **48**, 1–4.

Dent, A.J., Ramsay, J.D.F., Swanton, S.W., 1992. An EXAFS study of uranyl ion in solution and sorbed onto silica and montmorillonite clay colloids. *J. Colloid Interf. Sci.* **150** (1), 45–60.

Diaz-Arocas, P., Grambow, B., 1998. Solid-liquid phase equilibria of U(VI) in NaCl solutions. *Geochim. Cosmochim. Acta* **62** (2), 245–263.

Eliet, V., Grenthe, I., Bidoglio, G., 2000. Time-resolved laser-induced fluorescence of uranium (VI) hydroxo-complexes at different temperatures. *Appl. Spectrosc.* **54**, 99.

Elzinga, E.J., Tait, C.D., Reeder, R.J., Rector, K.D., Donohoe, R.J., Morris, D.E., 2004. Spectroscopic investigation of U(VI) sorption at the calcite–water interface. *Geochim. Cosmochim. Acta* **68** (11), 2437–2448.

Froideval, A., 2004. Chimie de l'uranium(VI) à l'interface solution/minéraux (quartz et hydroxide d'aluminium): expériences et caractérisations spectroscopiques. Phd Thesis, Université L. Pasteur, Strasbourg, France, 186 p.

Froideval, A., Del Nero, M., Barillon, R., Hommet, J., Mignot, G., 2003. pH-dependence of uranyl retention in the quartz/solution system—an XPS study. *J. Colloid Interf. Sci.* **266**, 221–235.

Gabriel, U., Charlet, L., Schläpfer, C.W., Vial, J.C., Brachmann, A., Geipel, G., 2001. Uranyl surface speciation on silica particles studied by time-resolved laser-induced fluorescence spectroscopy. *J. Colloid Interf. Sci.* **239**, 358–368.

Grenthe, I., Fuger, J., Konings, R.J.M., Lemire, R.J., Muller, A.B., Nguyen-Trung, C., Wanner, H., 1992. *Chemical Thermodynamics of Uranium*. Elsevier Science Publishers, North Holland, Amsterdam, 715 p..

Guillaumont, R., Fanghänel, T., Fuger, J., Grenthe, I., Neck, V., Palmer, D.A., Rand, M.H., 2003. *Update on the Chemical Thermodynamics of Uranium, Neptunium, Plutonium, Americium and Technicium*. Elsevier Science Publishers, North Holland, Amsterdam, 919 p..

Hennig, C., Reich, T., Dähn, R., Scheidegger, A.M., 2002. Structure of uranium sorption complexes at montmorillonite edge sites. *Radiochim. Acta* **90**, 653–657.

Hudson, E.A., Terminello, L.J., Viani, B.E., Denecke, M., Reich, T., Allen, P.J., Bucher, J.J., Shuh, D.K., Edelstein, N.M., 1999. The structure of U^{6+} sorption complexes on vermiculite and hydrobiotite. *Clays Clay Miner.* **47**, 439–457.

Kato, Y., Meinrath, G., Kimura, T., Yoshida, Z., 1994. A study of U(VI) hydrolysis and carbonate complexation by Time-Resolved Laser-Induced Fluorescence Spectroscopy (TRLFS). *Radiochim. Acta* **64**, 107–111.

Kim, C.S., Rytuba, J.J., Brown Jr., G.E., 2004. EXAFS study of mercury(II) sorption to Fe- and Al-(hydr)oxides. I. Effects of pH. *J. Colloid Interf. Sci.* **271**, 1–15.

Kirishima, A., Kimura, T., Tochiyama, O., Yoshida, Z., 2004. Speciation study on uranium hydrolysis at high temperatures and pressures. *J. Alloys Compd.* **374**, 277–282.

Kowal-Fouchard, A., Drot, R., Simoni, E., Ehrhardt, J.J., 2004. Use of spectroscopic techniques for uranium(VI)/montmorillonite interaction modeling. *Environ. Sci. Technol.* **38**, 1399–1407.

Lefèvre, G., Duc, M., Lepeut, P., Caplain, R., Fédoroff, M., 2002. Hydration of γ-alumina in water and its effects on surface reactivity. *Langmuir* **18**, 7530–7537.

May, H.M., Helmke, P.A., Jackson, M.L., 1979. Gibbsite solubility and thermodynamic properties of hydroxyaluminum ions in aqueous solutions at 25 °C. *Geochim. Cosmochim. Acta* **43**, 861–868.

McKinley, J.P., Zachara, J.M., Smith, S.C., Turner, G., 1995. The influence of uranyl hydrolysis and multiple site-binding reactions on adsorption of U(VI) to montmorillonite. *Clays Clay Miner.* **43** (5), 586–598.

Moll, H., Reich, T., Szabo, Z., 2000. The hydrolysis of dioxouranium(VI) investigated using EXAFS and ^{17}O-NMR. *Radiochim. Acta* **88** (7), 411–415.

Morris, D.E., Allen, P.G., Berg, J.M., Chisholm-Brause, C.J., Conradson, S.D., Donohoe, R.J., Hess, N.J., Musgrave, J.A., Tait, C.D., 1996. Speciation of uranium in Fernald soils by molecular spectroscopic methods: characterization of untreated soils. *Environ. Sci. Technol.* **30** (7), 2322–2330.

Morrison, S.J., Tripathi, V.S., Spangler, R.R., 1995. Coupled reaction/transport modeling of a chemical barrier for controlling uranium(VI) contamination in groundwater. *J. Contaminant Hydrol.* **17**, 347–363.

Moulin, C., Decambox, P., Moulin, V., Decaillon, J.G., 1995. Uranium speciation in solution by time-resolved laser-induced fluorescence. *Anal. Chem.* **67**, 348–353.

Moulin, C., Laszak, I., Moulin, V., Tondre, C., 1998. Time-resolved laser-induced fluorescence as a unique tool for low level uranium speciation. *Appl. Spectrosc.* **52**, 528.

Moyes, L.N., Parkman, R.H., Charnock, J.M., Vaughan, D.J., Livens, F.R., Hughes, C.R., Braithwaite, A., 2000. Uranium uptake from aqueous solution by interaction with goethite, lepidocrocite, muscovite and mackinawite: an X-ray absorption spectroscopy study. *Environ. Sci. Technol.* **34**, 1062–1068.

Murakami, T., Ohnuki, T., Isobe, H., Sato, T., 1997. Mobility of uranium during weathering. *Am. Mineral.* **82**, 888–899.

Navaza, A., Villain, F., Charpin, P., 1984. Crystal structures of the dicyclohexa-(18-crown-6) uranyl perchlorate complex and its hydrolysis product. *Polyhedron* **3** (2), 143–149.

Newville, M., 2001. IFEFFIT: interactive XAFS analysis and FEFF fitting. *J. Synchrotron Rad.* **8**, 322–324.

Newville, M., Ravel, B., Haskel, D., Rehr, J.J., Stern, A., Yacoby, Y., 1995. Analysis of multiple-scattering XAFS data using theoritical standards. *Phys. B* **208–209**, 154–156.

Nordstrom, D.K., May, H.M., 1996. Aqueous equilibrium data for mononuclear aluminum species. In: Sposito, G. (Ed.), *The Environmental Chemistry of Aluminum*. CRC, Lewis Publishers, Boca Raton, FL, pp. 9–80.

Payne, T.E., Davis, J.A., Waite, T.D., 1994. Uranium retention by weathered schists. The role of iron minerals. *Radiochim. Acta* **66/67**, 297–303.

Reich, T., Moll, H., Denecke, M.A., Geipel, G., Bernhard, G., Nitsche, H., 1996. Characterization of hydrous uranyl silicate by EXAFS. *Radiochim. Acta* **74**, 219–223.

Reich, T., Moll, H., Arnold, T., Denecke, M.A., Henning, C., Geipel, G., Bernhard, G., Nitsche, H., Allen, P.G., Bucher, J.J., Edelstein, N.M., Shuh, D.K., 1998. An EXAFS study of uranium(VI) sorption onto

silica gel and ferrihydrite. *J. Electron Spectrosc. Related Phenomena* **96**, 237–243.

Sylwester, E.R., Hudson, E.A., Allen, P.G., 2000. The structure of uranium(VI) sorption complexes on silica, alumina and montmorillonite. *Geochim. Cosmochim. Acta 64* **14**, 2431–2438.

Taylor, J.C., Hurst, H.J., 1971. The hydrogen atom localisations in the α and β forms of uranyl hydroxide. *Acta Cryst. B* **27**, 2018.

Thompson, H.A., Brown Jr., G.E., Parks, G.A., 1997. XAFS spectroscopic study of uranyl coordination in solids and aqueous solution. *Am. Min.* **82**, 483–496.

Torrero, M.E., Casas, I., de Pablo, J., Sandino, M.C.A., Grambow, B., 1994. A comparison between unirradiated UO_2(s) and schoepite solubilities in 1 M NaCl medium. *Radiochim. Acta* **66/67**, 29–35.

Turner, G.D., Zachara, J.M., McKinley, J.P., Smith, S.C., 1996. Surface-charge properties and UO_2^{2+} adsorption of a subsurface smectite. *Geochim. Cosmochim. Acta* **60** (18), 3399–3414.

Wahlgren, U., Moll, H., Grenthe, I., Schimmelpfennig, B., Maron, L., Vallet, V., Gropen, O., 1999. Structure of uranium(VI) in strong alkaline solutions. A combined theoretical and experimental investigation. *J. Phys. Chem. A* **103** (41), 8257–8264.

Waite, T.D., Davis, J.A., Payne, T.E., Waychunas, G.A., Xu, N., 1994. Uranium(VI) adsorption to ferrihydrite. *Geochim. Cosmochim. Acta 58* **24**, 5465–5478.

Walter, M., Arnold, T., Geipel, G., Scheinost, A., Bernhard, G., 2005. An EXAFS and TRLFS investigation on uranium(VI) sorption to pristine and leached albite surfaces. *J. Colloid Interf. Sci.* **282**, 293–305.

Wang, P., Anderko, A., Turner, D.R., 2001. Thermodynamic modeling of the adsorption of radionuclides on selected minerals. *I. Cations. Ind. Eng. Chem. Res.* **40**, 4428–4443.

Weller, M.T., Light, M.E., Gelbrich, T., 2000. Structure of uranium(VI) dehydrate $UO_3{\cdot}2H_2O$, synthetic meta-schoepite $(UO_2)_4O(OH)_6{\cdot}5H_2O$. *Acta Cryst. B* **56**, 577–583.

Wijnja, H., Schulthess, C.P., 1999. ATR-FTIR and DRIFT spectroscopy of carbonate species at the aged γ-Al_2O_3/water interface. *Spectrochim. Acta Part A* **55**, 861–872.